applied sciences

MDPI

Article

Experimental and Computational Vibration Analysis for Diagnosing the Defects in High Performance Composite Structures Using Machine Learning Approach

Lakshmipathi Jakkamputi [1], Saravanakumar Devaraj [2], Senthilkumar Marikkannan [1], Sakthivel Gnanasekaran [2], Sivakumar Ramasamy [1], Jegadeeshwaran Rakkiyannan [2,*] and Yigeng Xu [3]

[1] School of Mechanical Engineering, Vellore Institute of Technology, Chennai 600127, India
[2] Centre for Automation, Vellore Institute of Technology, Chennai 600127, India
[3] Centre for Aeronautics, Cranfield University, Cranfield MK43 0AL, UK
* Correspondence: jegadeeshwaran.r@vit.ac.in; Tel.: +91-44-3993-1335

Abstract: Delamination in laminated structures is a concern in high-performance structural applications, which challenges the latest non-destructive testing techniques. This study assesses the delamination damage in the glass fiber-reinforced laminated composite structures using structural health monitoring techniques. Glass fiber-reinforced rectangular laminate composite plates with and without delamination were considered to obtain the forced vibration response using an in-house developed finite element model. The damage was diagnosed in the laminated composite using machine learning algorithms through statistical information extracted from the forced vibration response. Using an attribute evaluator, the features that made the greatest contribution were identified from the extracted features. The selected features were further classified using machine learning algorithms, such as decision tree, random forest, naive Bayes, and Bayes net algorithms, to diagnose the damage in the laminated structure. The decision tree method was found to be a computationally effective model in diagnosing the delamination of the composite structure. The effectiveness of the finite element model was further validated with the experimental results, obtained from modal analysis using fabricated laminated and delaminated composite plates. Our proposed model showed 98.5% accuracy in diagnosing the damage in the fabricated composite structure. Hence, this research work motivates the development of online prognostic and health monitoring modules for detecting early damage to prevent catastrophic failures of structures.

Keywords: machine learning; statistical features; fault diagnosis; delamination; composites; vibration

Citation: Jakkamputi, L.; Devaraj, S.; Marikkannan, S.; Gnanasekaran, S.; Ramasamy, S.; Rakkiyannan, J.; Xu, Y. Experimental and Computational Vibration Analysis for Diagnosing the Defects in High Performance Composite Structures Using Machine Learning Approach. *Appl. Sci.* **2022**, *12*, 12100. https://doi.org/10.3390/app122312100

Academic Editor: Paolo Visconti

Received: 20 September 2022
Accepted: 23 November 2022
Published: 26 November 2022

Publisher's Note: MDPI stays neutral with regard to jurisdictional claims in published maps and institutional affiliations.

Copyright: © 2022 by the authors. Licensee MDPI, Basel, Switzerland. This article is an open access article distributed under the terms and conditions of the Creative Commons Attribution (CC BY) license (https://creativecommons.org/licenses/by/4.0/).

1. Introduction

Laminated composite structures that are currently used for structural applications, such as windmill propeller blades, rotorcraft blades, marine propeller blades, and turbine blades, are manufactured by stacking fiber-reinforced lamina in a sequence of interest to provide high strength, stiffness, and stability. These structures are more vulnerable to damage such as the de-bonding of laminate or delamination that originates from dynamic loads, impact loads, excessive deformations during the service, or poor manufacturing methods [1]. Delamination is the most common and severe form of damage that reduces the stiffness, stability, and load-carrying capacity of the structure. Delamination takes place inside the composite structure without being evident from external surfaces, resulting in matrix breakage and leading to deteriorating mechanical properties. Especially under dynamic loads, delamination can pose a severe threat to the reliability, integrity, and usability of laminate structures without any visible indications. Furthermore, the delamination in composites is usually difficult to identify in rea time,

even with cost-intensive and time-consuming non-destructive testing (NDT) techniques [2]. Henceforth, efficient inspection methods and early detection are necessary to prevent catastrophic failures of structures.

Structural health monitoring (SHM) is a state-of-the-art technology to monitor the condition and diagnose the damage and faults in machine and structural components. SHM uses advanced techniques, such as the vibration-based method [3–5], fiber Bragg grating (FBG) [5], acoustic emissions (AE) [6], impedance-based method [7], Lamb wave methods [8], etc. The use of the FBG technique is limited in the real-time health monitoring of the composite structures, because of the difficulty in embedding the optical fibers during fabrication. Furthermore, very fine grids of FBGs are necessary to capture changes in a structure [9]. The AE method cannot be used to detect damage in a structure unless the damage generates and propagates acoustic signals. Moreover, skilled personnel are required to differentiate the AE signal from the surrounding noise. On the other hand, impedance-based and Lamb wave techniques require a large number of transducers to precisely detect the location and size of the damage [10]. Compared with these approaches, the vibration-based method is generally proposed to diagnose the structural faults or damage, as the damage that is present in a laminated composite structures causes variations in dynamic behavior and the modal parameters, by which the incidence of faults can be detected [11].

Vibration signatures contain vital information regarding the structural health condition, such as the source of failure and its severity [12]. By analyzing the vibration signatures and the damage present in the laminated composite structures that cause variations in the dynamic behavior and modal parameters, the incidence of faults can be detected. Maia et al. reviewed the damage diagnostic techniques in composite structures using vibration-based methods. This is achieved through a real-time monitoring system by adopting well-developed signal processing techniques [13]. Hence, the vibration signal analysis was chosen to monitor the health status of the composite plates.

Vibration signals are generally captured using the accelerometer sensor in time, frequency, and time-frequency domains [14]. The frequency and time-frequency domains require essential mathematical functions to process the signal. Due to this time and computational complexity, the time-domain format is generally used for fault diagnosis studies. The captured time-domain data consists of cumulative information about the nature of the structure. This information has to be properly analyzed to decide on the structure. Hence, vibration signal analysis is essential for extracting meaningful information. Vibration signals can be analyzed using spectral analysis, wavelet analysis, waveform analysis, etc. Spectral analysis transforms the signal from the time domain to the frequency domain using a fast Fourier transform. However, spectral analysis applies only to stationary signals. Waveform analysis helps to provide fundamental information about fault locations. However, this analysis requires complex algorithms for detecting faults [15]. Envelop analysis detects impacts with very low energy often hidden by other vibration signals [16]; however, it is very difficult to identify the small variations in the signal. All these shortfalls can be overcome by adopting a statistical feature analysis. Statistical analysis is the process of collecting and analyzing data to identify patterns and trends. Talab et al. reported a novel statistical feature analysis for facial recognition applications [17]. Khairnar et al. studied tool insert conditions using statistical features extracted from vibration signals [18]. Bansal et al. used statistical feature extraction for developing an iris recognition system [19]. Li et al. used statistical features for the diagnosis of a rolling element bearing [20]. From the literature, it is evident that statistical features help to gain deeper insights about our data for fault identification. Hence, we propose using statistical analysis to diagnose damage in fiber-reinforced laminated composite structures.

A set of statistical features can be extracted from the time-domain vibration response for both laminated and delaminated structures. All the extracted information is not necessarily required for accurate classification. Hence, the selection of highly contributing

features is necessitated. Features are generally selected using principal component analysis (PCA), decision tree (DT), attributes evaluator, etc. Song et al. suggested using CA for selecting the features [21]. PCA is highly sensitive and not appropriate for data sets that have incomplete information [22]. A decision tree (DT), which is a graphical tree-based structure, can be used for selecting contributing features. Sugumaran et al. reported that a decision tree was effectively used for feature selection in bearing fault diagnosis [23]. However, the order of features may affect classification accuracy. Hence, we need to identify the order of contributing features. This can be achieved through the attribute evaluator, which eliminates non-contributing features [24].

Feature classification is the most important step in machine learning (ML). Many researchers have applied various ML algorithms to classify the features for diagnosing faults in many applications. The Bayesian family (naive Bayes and Bayes net) and random forest methods have been studied by researchers due to their computational effort and complexity level. Anuja et al. made a comparative study of different classification algorithms and found that the decision tree method was an effective choice for fault diagnosis study [25]. Li et al. used an improved decision tree for diagnosing faults in a VRF system with 98% classification accuracy [26]. Jegadeeshwaran and Sugumaran obtained 97% classification accuracy in brake fault diagnosis using a decision tree algorithm [27]. Compared with other algorithms, the decision tree requires less effort for data preparation during pre-processing and does not require normalization of data. Naive Bayes is a multi-class classifier that is used for making predictions in real-time. Akher et al. used a naive Bayes classifier for detecting faults in a transmission line [28]. Veronika et al. obtained 98.8% classification accuracy with a naive Bayes classifier model for gear fault diagnosis [29]. Kaplan et al. achieved 100% accuracy with both the naive Bayes and Bayes net classifier algorithms in bearing fault diagnoses [30]. It is easy and fast to predict the class of the test data set with the Bayesian algorithm. It also performs well in multi-class predictions. Akar et al. used a random forest algorithm for multispectral image classification [31]. Paul et al. proposed an improved random forest classifier that performs a classification with a minimum number of trees and achieved maximum classification accuracy [32]. Referring to the above literature, one can easily understand that ML algorithms have been used for various applications that include rotating machine elements. There are many conventional approaches for detecting faults in a laminated composite [33–35]. However, there is limited literature on inspecting the impact response produced on static elements using machine learning. Hence, an effort has been made to categorize delaminated composites using machine learning algorithms such as decision tree, naive Bayes, Bayes net, and random forest.

In the proposed research work, delamination damage in glass fiber-reinforced laminated composite structures are diagnosed using prognostic and health management techniques as per the following sequential procedures. Fiber-reinforced rectangular laminated and delaminated polymer composite plates have been considered to obtain the forced vibration response using the finite element analysis (FEA). The energy functional corresponding to the laminated and delaminated structures are obtained in terms of kinetic energy and potential energy using first-order shear deformation theory (FSDT). Further, the governing differential equations of motion are obtained in terms of the finite element formulations by extremizing the energy functional. The time-domain vibration signals of the delaminated and laminated composite structures are acquired using an in-house developed finite element program using MATLAB®. The statistical information that is extracted from the forced vibration response is used to diagnose the damage in the laminated composite plates using machine learning algorithms. The greatest contributing features are identified from the extracted features through the attribute evaluator to reduce computational time. The selected information is further used to diagnose the delamination damage in the composite structure using various machine learning approaches, such as random forest, naive Bayes, decision tree, and Bayes net algorithms. The effectiveness of the finite element model is further validated with the experimental

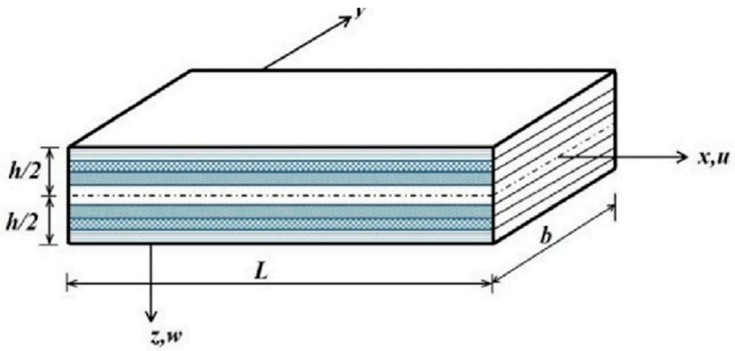
results obtained from modal analysis using the fabricated laminated and delaminated composite plates.

2. Mathematical Modelling

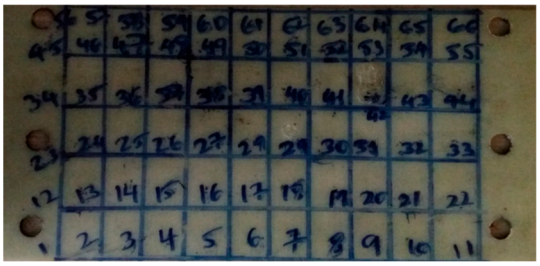
2.1. Theoretical Modeling

2.1.1. Laminate Composite

The laminated and delaminated glass fiber-reinforced polymer composite structure configurations with photographs are shown in Figure 1 for the mathematical modeling of transverse vibration response in the time domain. The laminate structure is assumed to have perfect bonding between all layers, whereas the delaminate structure is assumed to be debonding in the central plane, with a size of 100 × 100 mm placed symmetrically at the center of the plate. The length, breadth, and thickness of the laminated and delaminated composite structures are assumed to be 'L', 'b', and 'h', respectively.



(**a**) Representation of laminate configuration.



(**b**) Photograph of the laminate structure.



(**c**) Photograph of delaminate structure.

Figure 1. Composite plate configuration.

The force and moment resultants associated with the mid-plane strains and curvatures of the laminated composite plate is expressed as

$$N = A\varepsilon_0 + Bk$$

$$M = B\varepsilon_0 + Dk \quad (1)$$

$$Q = K_s A^s \gamma_0$$

where $N = \begin{Bmatrix} N_{xx} \\ N_{yy} \\ N_{xy} \end{Bmatrix}$, $\mathrm{M} = \begin{Bmatrix} M_{xx} \\ M_{yy} \\ M_{xy} \end{Bmatrix}$, and $Q = \begin{Bmatrix} Q_y \\ Q_x \end{Bmatrix}$ are in-plane force, moment, and transverse shear force resultants, respectively. A, D, B, and A^s denote extensional stiffness, bending stiffness, extensional–bending stiffness, and transverse shear stiffness, which are given by [36].

The strain energy (U) and kinetic energy (K) are expressed in terms of in-plane and transverse displacements, rotations of transverse normal, and out-of-plane shear strains,

whereas virtual work done (V) is expressed in terms of transverse load, external forces and moments given by [37].

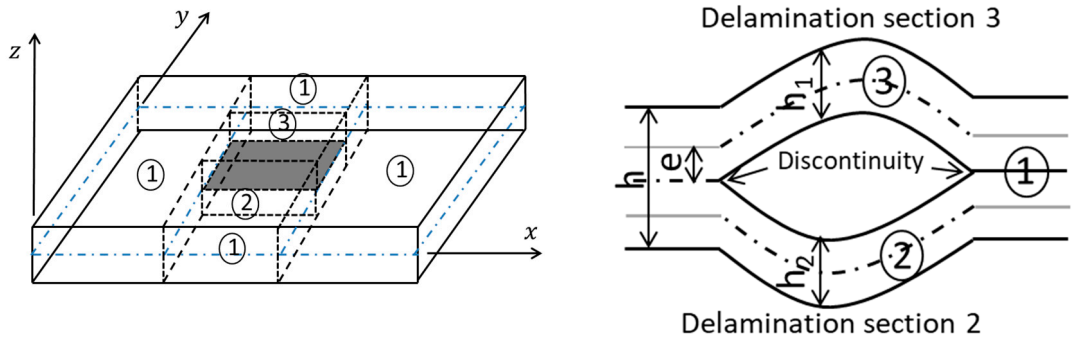
The governing differential equations of motion for the FRP composite plate are obtained by using Hamilton's principle, as

$$\begin{gathered}\frac{\partial N_{xx}}{\partial x}+\frac{\partial N_{xy}}{\partial y}-I_0\ddot{u}_0-I_1\ddot{\emptyset}_x=0\\ \frac{\partial N_{yy}}{\partial y}+\frac{\partial N_{xy}}{\partial x}-I_0\ddot{v}_0-I_1\ddot{\emptyset}_y=0\\ \frac{\partial M_{xx}}{\partial x}+\frac{\partial M_{xy}}{\partial y}-Q_x-I_0\ddot{\emptyset}_x-I_1\ddot{u}_0=0\\ \frac{\partial M_{yy}}{\partial y}+\frac{\partial M_{xy}}{\partial x}-Q_y-I_0\ddot{\emptyset}_y-I_1\ddot{v}_0=0\\ \frac{\partial Q_x}{\partial x}+\frac{\partial Q_y}{\partial y}+q-I_0\ddot{w}_0=0\end{gathered} \tag{2}$$

where u_0 and v_0, w, and $\emptyset_x$ and $\emptyset_y$ are the in-plane displacements, transverse deflection, and rotations of transverse normal, respectively.

2.1.2. Delamination Formulation

The deformation field for the 2D delamination laminated structure is obtained based on the FSDT model, as discussed earlier. The structure with delamination was divided into the intact region (1), lower delamination region (2), and upper delamination region (3), as shown in Figure 2. The lower and upper delaminated layers are assumed to undergo deformation without contact with each other at the center delamination boundary, as shown in Figure 2b. Global coordinates *(X, Y, Z)* are assigned to the center delamination plate, as shown in Figure 2a. The mid-plane deformation field (u_0, v_0, w_0) of the intact region (Segment 1) is considered to be different from the mid-plane deformation field $({u_0}^L, {v_0}^L, {w_0}^L)$ of the lower delamination region (Section 2) and the mid-plane deformation field $({u_0}^U, {v_0}^U, {w_0}^U)$ of the upper delamination region (Section 2). The rotations of transverse normal of intact, lower delamination, and upper delamination regions are represented as $\emptyset_x$ and $\emptyset_y$, ${\emptyset_x}^L$ and ${\emptyset_y}^L$, and ${\emptyset_x}^U$ and ${\emptyset_y}^L$, respectively. The thickness of the intact, lower delamination, and upper delamination regions are considered to be h, h_1, and h_2, respectively.



(**a**) Delaminated structure (**b**) Discontinuity in Delamination

Figure 2. Geometry of laminate composite structure with center delamination.

The deformation field of the intact region (Segment 1) is given by

$$u = \{u_0{}^i\} + z\{\emptyset\} \tag{3}$$

The deformation field of the delamination region (Segments 1 and 2) is given by

$$u^{L,U} = \{u_0{}^{L,U}\} + z\{\emptyset^{L,U}\} \tag{4}$$

where $u_0{}^i = \begin{Bmatrix} u_0 \\ v_0 \\ w_0 \end{Bmatrix}$, $u_0{}^{L,U} = \begin{Bmatrix} u_0{}^{L,U} \\ v_0{}^{L,U} \\ w_0{}^{L,U} \end{Bmatrix}$, and $\emptyset = \begin{Bmatrix} \emptyset_x{}^{L,U} \\ \emptyset_y{}^{L,U} \\ 0 \end{Bmatrix}$

The upper and lower delamination region boundary elements should be connected to single elements of the laminated region along the interface of intact and delaminated regions. It is essential to impose continuity conditions between the elements of intact and delamination regions. To ensure the continuity of the displacement field across the thickness of the plate at such element nodes, the displacement field of the neutral plane of the lower or upper delaminated portion at the interface boundary should be essentially identical to that of the element nodes adjacent to the planes in the intact region. Therefore, the continuity equations at the interface are given by

$$\begin{aligned} u_0{}^{L,U} &= \{u_0\} + e\{\emptyset\}, \\ v_0{}^{L,U} &= \{v_0{}^{L,U}\} + e\{\emptyset\}, \\ w_0{}^{L,U} &= w_0, \\ \emptyset_x{}^{L,U} &= \emptyset_x, \\ \emptyset_y{}^{L,U} &= \emptyset_y \end{aligned} \tag{5}$$

where $e = \frac{h - h_{1,2}}{2}$.

Therefore, from the Equation (5), the deformation field of the lower and upper delamination region at the delamination boundary can be written in terms of the mid-plane deformation of the intact laminate structure.

$$\begin{Bmatrix} u_0{}^{L,U} \\ v_0{}^{L,U} \\ w_0{}^{L,U} \\ \emptyset_x{}^{L,U} \\ \emptyset_y{}^{L,U} \end{Bmatrix} = \begin{bmatrix} 1 & 0 & 0 & e & 0 \\ 0 & 1 & 0 & 0 & e \\ 0 & 0 & 1 & 0 & 0 \\ 0 & 0 & 0 & 1 & 0 \\ 0 & 0 & 0 & 0 & 1 \end{bmatrix} \begin{Bmatrix} u_0 \\ v_0 \\ w_0 \\ \emptyset_x \\ \emptyset_y \end{Bmatrix} \tag{6}$$

The governing differential equations of motion for the FRP composite plate with delamination are obtained similarly to Equation (2).

2.2. Computational Modeling

FEA Modeling

The laminated and delaminated composite structures were modeled using an eight-node serendipity element with five degrees of freedom associated at each node (Figure 3). The interpolation functions ($\widehat{N}_i$) of the deformation field for the finite element formulations are derived using the iso-parametric formulations. The deformation field in the typical element of the intact and laminated composite structure is expressed in terms of Lagrange interpolation functions (in natural coordinates) and nodal degrees of freedom (DOF), as

$$\begin{Bmatrix} u_0 \\ v_0 \\ w_0 \\ \emptyset_x \\ \emptyset_y \end{Bmatrix} = \begin{bmatrix} \widehat{N}_i & 0 & 0 & 0 & 0 \\ 0 & \widehat{N}_i & 0 & 0 & 0 \\ 0 & 0 & \widehat{N}_i & 0 & 0 \\ 0 & 0 & 0 & \widehat{N}_i & 0 \\ 0 & 0 & 0 & 0 & \widehat{N}_i \end{bmatrix} \begin{Bmatrix} u_{0i} \\ v_{0i} \\ w_{0i} \\ \emptyset_{xi} \\ \emptyset_{yi} \end{Bmatrix}$$

$$\begin{Bmatrix} u_0{}^{L,U} \\ v_0{}^{L,U} \\ w_0{}^{L,U} \\ \emptyset_x{}^{L,U} \\ \emptyset_y{}^{L,U} \end{Bmatrix} = \begin{bmatrix} \widehat{N}_i & 0 & 0 & 0 & 0 \\ 0 & \widehat{N}_i & 0 & 0 & 0 \\ 0 & 0 & \widehat{N}_i & 0 & 0 \\ 0 & 0 & 0 & \widehat{N}_i & 0 \\ 0 & 0 & 0 & 0 & \widehat{N}_i \end{bmatrix} \begin{Bmatrix} u_{0i}{}^{L,U} \\ v_{0i}{}^{L,U} \\ w_{0i}{}^{L,U} \\ \emptyset_{xi}{}^{L,U} \\ \emptyset_{yi}{}^{L,U} \end{Bmatrix} \tag{7}$$

where $i = 1,2, \ldots, 8$

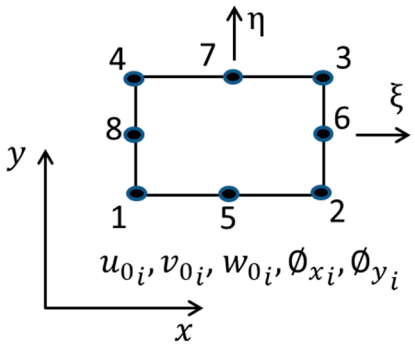


Figure 3. Plate element.

The governing equations of motion are obtained in terms of finite element equations by substituting Equation (7) into the variational principle as

$$[M]^e\{\ddot{d}\}^e + [K]^e\{d\}^e = \{f\}^e \tag{8}$$

where $[K]^e$, $[M]^e$, $\{f\}^e$, and $\{d\}^e$ are element stiffness, mass matrix, force vector, and deformation vector, respectively, which are described in the appendix. Assembling of

the element stiffness and mass matrix of all the elements results in a governing equation of motion for the laminated and delaminated composite structure, as given below.

$$[M]\{\ddot{d}\} + [K]\{d\} = \{f\} \quad (9)$$

$[K]$, $[M]$, $\{f\}$, and $\{d\}$ are global stiffness, mass matrix, force vector, and deformation vector, respectively.

The solution for Equation (9) can be expressed in terms of normal modes (X) and principal coordinates (q), as

$$\{d\} = [X]\{q(t)\} \quad (10)$$

Equation (10) uncouples Equation (9), so that we can obtain the second-order uncoupled differential equations, as shown below.

$$[I]\{\ddot{q}\} + [\ddots\ {\omega_i}^2\ \ddots]\{q\} = \{Q\} \quad (11)$$

where ω_i is the natural frequency of i^{th} mode and $\{Q\}$ is the generalized force vector in terms of the principal coordinates.

Once the generalized deformation vector $q(t)$ is found from Equation (10), the physical deformation vector can be obtained using Equation (11).

2.3. Machine Learning Modelling

The vibration response acquired from the developed FEA model is processed to obtain statistical information. The combination of this information is used to extract the damage information in the laminated composite structure using a machine learning model.

2.3.1. Feature Extraction

The process of decomposing the signal for extracting information is called feature extraction. The statistical parameters that were extracted from both the simulated and experimental vibration signals using the visual basic code [8].

2.3.2. Feature Selection

The initial set of raw features can be redundant and too large manage. Therefore, selecting a subset of features is an important step in improving generalization and interpretability. The selection of features in classifying the damage in the composite structures is very critical in machine learning techniques. In the present study, the feature selection was performed using an attribute evaluator. The attribute evaluator ranks each contributing feature. Based on this ranking, the effect of contributing features is evaluated using the effect of the number of features studied.

2.3.3. Feature Classification

A classifier is an algorithm that performs the classification of a dataset. The fundamental purpose of a classification algorithm is to predict the output for categorical data. A classification algorithm uses a supervised learning technique to determine the category of new observations through a trained data set. A program learns from the dataset, and then classifies fresh observations into one of several classes (targets/labels). Various machine learning classifiers, such as naive Bayes, Bayes net, support vector machines, and others can be used to classify the specified features.

3. Experimental Study

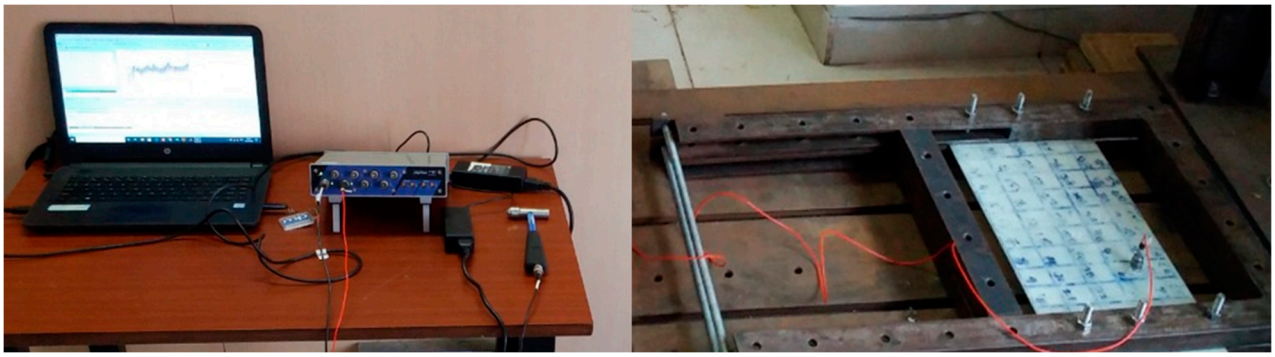
The efficacy of the mathematical model developed using finite elements to measure the forced vibration response of an intact and delaminated composite structure was studied by comparing the MATLAB® simulated transverse deflections in the time domain with that of laboratory experimental results. The intact and delaminated fi-

ber-reinforced laminated structures were fabricated using a vacuum-assisted hand-lay-up process. First, peel fly fabric treated with a releasing agent was laid upon the mold surface to provide a smooth finish on the structure surface. E-glass unidirectional woven fabric of 225 g/m² was placed over the peel ply, and then the calculated amount of LY556 epoxy resin with HY951 was evenly applied over the fiber surface. The lay-up was continued to obtain a stacking sequence of [0°/90°]4 s with sixteen layers. After obtaining the required sequence of lay-up, the peel ply and breather fabric were laid over the lay-up stack. The entire setup was placed inside a vacuum bag, which was sealed with a sealant. Initially, the laminated stack was cured at vacuum pressure and room temperature for one hour. Later, the laminate was placed in an oven where the temperature was raised to 70 °C at a controlled rate of 1 °C/min. In the next stage, the laminate was kept at 70 °C for two hours. Finally, the laminated composite structure was allowed to cure further for one day at room temperature. The prototypes were cut into 400 mm length × 200 mm width. The delamination in the composite structure was obtained by inserting 100 × 100 mm Teflon film symmetrically in the central plane during the fabrication process. Both the composite structures maintained an identical volume fraction of 0.4. Figure 1a,b shows the fabricated laminated and delaminated composite structures. The thickness of the laminated and delaminated structures was measured to be 4.158 and 4.032 mm, respectively. The mechanical properties of the unidirectional laminate ply are presented in Table 1.

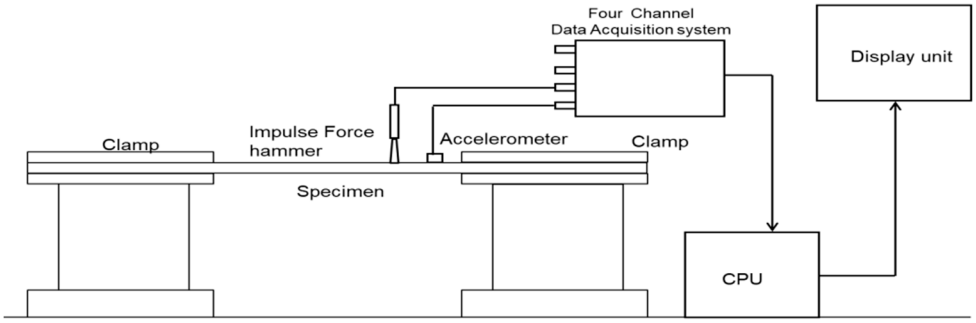
Table 1. Mechanical properties of the unidirectional fiber-reinforced composite lamina.

Fiber-Reinforced Composite Lamina	
V_f	0.4
$E_{11}(Gpa)$	30.2
$E_{22}(Gpa)$	6.8
v_{12}	0.269
$G_{12}(Gpa)$	2.8
$G_{23}(Gpa)$	2.51
$\rho_c(kg/m^3)$	1745

The schematic diagram of the experimental setup used to obtain the time-domain response of the laminated and the delaminated composite structure is shown in Figure 4. The composite structures were divided into fifty rectangular elements and sixty-six nodes to measure the time-domain response and impact force at the various nodes. The impact hammer was used to excite all the nodes of the composite plate. A uni-axis accelerometer (50 g/100 mV/g sensitivity) was fixed at the location of 234 × 134 mm from the left end bottom corner of the plate to record the acceleration in the time domain due to impact excitation at all the nodes of the plate. The time-domain response (h_{ij}) acquired using the four-channel data acquisition system represents the response at the eighth node due to the impact excitation at the j^{th} node of the laminated and delaminated composite plates. The experiments were performed in a temperature-controlled environment using air-conditioning. The temperature was set to 27 °C during the transverse response extraction of the intact and delaminated composites.



(**a**) Photograph of experimental setup.



(**b**) Schematic diagram of experimental setup.

Figure 4. Experimental setup.

4. Results and Discussion

4.1. Validation

The effectiveness of the developed finite element formulation was further verified by comparing the results available in the literature. Babu et al. [37] evaluated the natural frequencies of a non-uniform fiber-reinforced polymer laminated composite structure by considering ply orientations [0/90]8s at the right end and [0/90] at the left end, respectively. The mechanical and geometrical properties considered for the composite fiber lamina of all these configurations were E_1 = 30.2 GPa, E_2 = 6.8 Gpa, v_{12} = 0.269, G_{12} = 2.68 Gpa, ρ_c = 1745 kg/m^3, and a ply thickness of 0.19 mm, and resin pocket properties were E = 3.45, v = 0.3, G = 1.33 GPa, and ρ = 1200 kg/m^3. Table 2 compares the natural frequencies of the tapered laminated composite plate for (1,1), (1,2), and (2,1) modes under CFFF end conditions for the tapered configuration, by using the present finite element formulations with the results presented in Babu et al. [38]. Referring Table 2, the natural frequencies evaluated by the present FEM had a very close agreement with those presented in Babu et al.

Table 2. Comparison of the natural frequencies of a tapered composite plate derived by utilizing the present FEM with those presented in [38].

Modes (m,n)	Natural Frequencies (Hz)				% Deviation	
	Laminated Plate		Delaminated Plate			
	Ref. [38]	Present	Ref. [38]	Present	Laminated Plate	Delaminated Plate
1,1	21.1	20.8	20.6	20.1	1.42	2.49

1,2	39.4	40.4	38.2	39.1	2.54	2.3
2,1	102.2	100.4	97.5	96.6	1.76	0.93

The time-domain signals were obtained using a finite element code through MATLAB®. Two conditions of the composite plates, namely laminated and delaminated plates, were considered for the study. Forty nodes were arbitrarily selected and the corresponding time-domain signatures were simulated. Similarly, the laminated and delaminated composite plates were fabricated as shown in Figure 1a,b. The corresponding vibration signals were acquired from the composite plates using the accelerometer sensors. Figure 5 shows the time-domain response of the laminated and delaminated structures using numerical and experimental studies.

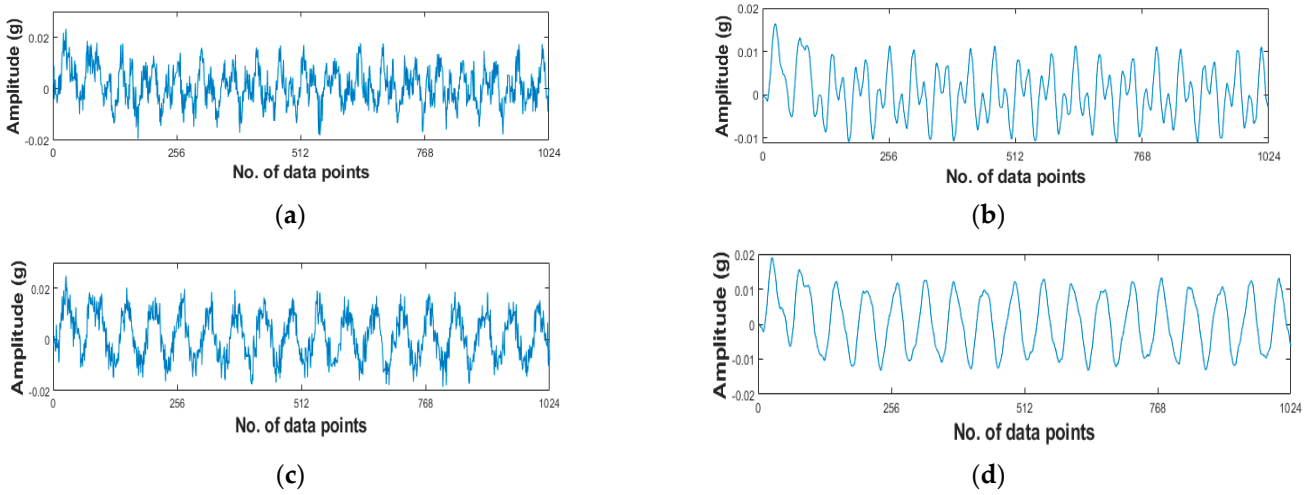


Figure 5. Vibration response of composite plates. (**a**) Experimental response of the laminated composite plate. (**b**) Finite element response of the laminated composite plate. (**c**) Experimental response of the delaminated composite plate. (**d**) Finite element response of the delaminated composite plate

4.2. Feature Extraction and Selection

The raw vibration signals were decomposed for extracting vital information as features. Thirteen sets of vital statistical information were mined from the simulated vibration signals. Tables 3 and 4 show the sample feature values extracted from the simulated and experimental vibration signals.

Table 3. Extracted features from the simulated data.

Mean	Standard Error	Median	Std. Deviation	Sample Variance	Kurtosis	Skewness	Range	Minimum	Maximum	Condition
0.01	0.36	−0.05	11.41	130.25	4.09	0.12	136.7	−73.65	0.01	LM
0.01	0.33	−0.05	10.53	110.98	3.77	0.07	122.3	−65.36	0.01	LM
0.00	0.27	−0.05	8.56	73.32	3.92	0.07	103.3	−57.21	0.00	LM
0.01	0.36	−0.05	11.41	130.25	4.09	0.12	136.7	−73.65	0.01	DLM
0.01	0.33	−0.05	10.53	110.98	3.77	0.07	122.3	−65.36	0.01	DLM
0.00	0.27	−0.05	8.56	73.32	3.92	0.07	103.3	−57.21	0.00	DLM

Table 4. Extracted features from the experimental data.

Mean	Standard Error	Median	Std. Deviation	Sample Variance	Kurtosis	Skewness	Range	Minimum	Maximum	Condition
0.04	0.42	−0.05	13.56	183.87	2.72	0.20	135.7	−68.17	67.58	LM
0.00	0.32	−0.05	10.10	101.99	3.18	0.43	94.76	−40.38	54.38	LM
0.03	0.38	−0.05	12.26	150.21	1.70	0.09	113.3	−56.39	56.94	LM

−0.05	0.05	−0.05	1.49	2.23	20.74	−1.45	24.74	−15.66	9.08	DLM
−0.04	0.11	0.00	3.42	11.69	7.86	−0.70	42.82	−24.79	18.04	DLM
−0.04	0.12	−0.04	3.93	15.47	14.56	−1.04	59.90	−38.31	21.59	DLM

All the features may not be required for classification. Hence, feature selection was initiated using the attribute evaluator and the effect of the number of features studied. The attribute evaluator ranks the contributing features. The first feature suggested by the attribute evaluator was selected and classified by the considered algorithms. The corresponding accuracy was noted. Then, the top two ranked features were selected for classification and the corresponding accuracy was noted. In the same way, all the features were clubbed one by one based on their ranking, and their corresponding accuracies are noted in Table 5. Referring to Table 5, all the algorithms produced the maximum classification accuracy with the top five feature combinations. These were the (1) Mean, (2) Standard error, (3) Sample variance, (4) Kurtosis, and (5) Skewness. However, the decision tree and naive Bayes algorithms produced the maximum accuracy with the top four features. Based on model-building time, the decision tree algorithm is suggested for further study.

Table 5. Effect of the number of features on classification accuracy—simulated data.

No. of Features	Classification Accuracy (%)			
	C4.5 Decision Tree	Random Forest	Naive Bayes	Bayes Net
1	56.00	54.25	57	47.5
2	80.90	80	86.25	84.36
3	90.72	96.25	88.75	87.45
4	100	98	100	96.25
5	100	100	99.0	100
6	100	99.12	98.2	99.4
7	98.2	98.5	97.9	98.5
8	97.9	98.5	97.1	97.7
9	96.4	97.2	96.2	96.6
10	95.2	96.3	95.1	95.9
11	95.2	96.3	94.9	94.2
12	94.9	96.3	94.3	94.6

4.3. Feature Classification

The decision tree classifier model was trained with the selected number of statistical features (mean, sample variance, standard error, and kurtosis) that were selected by the attribute evaluator. The trained model was tested and validated using a 10-fold cross-validation. The obtained results are disclosed in the form of a matrix known as the "confusion matrix" (Table 6).

Referring to Table 6, the first row denotes the data related to the laminated composite plates (LAM) and the second row represents the data relevant to delaminated composite plates. The first element in the first column represents the correctly classified elements. Among the 40 laminated composite plate data, all were correctly classified. Hence, there was no misclassification. The second element in the second column represents the data points corresponding to the delaminated plate (DLAM). In this case, all 40 data points were also correctly classified and none were misclassified. Among all 80 simulated data points, all 80 were correctly categorized. Hence, the classification accuracy with the DT algorithm is 100%. The time taken to build the model was 0.01 s.

Table 6. Confusion matrix for decision tree with simulated data.

Category	LAM	DLAM
LAM	40	0
DLAM	0	40

LAM: Laminated; DLAM: Delaminated plate.

Summary of the classifier results:

Correctly Classified Instances	100 (100%)
Incorrectly Classified Instances	0 (0%)
Kappa statistic	1
Mean absolute error	0
Root mean squared error	0
Relative absolute error	0
Coverage of cases (0.95 level)	100%
Mean rel. region size (0.95 level)	50%
Total Number of Instances	100

4.4. Experimental Validation

An experimental study was carried out for validating the proposed decision tree model. As per the proposed design, the laminated and delaminated composite plate was fabricated. Both laminated and delaminated sheets were fitted on a workbench and the frequency response in the time domain was acquired. From the time-domain response, the statistical information was extracted. Then feature selection process was carried out using the effect of the number of feature study. Table 7 shows the effect of number of features study on the classification accuracy.

Referring to Table 7, DT produced 98% maximum accuracy with the experimental data. Table 8 shows the confusion matrix for the experimental data. Among the total 100 experimental data, 98 data were correctly classified with an overall accuracy level as 98%. The decision tree uses a confidence factor of 0.25.

Table 7. Effect of the number of features on classification accuracy—Experimental data.

No. of Features	Classification Accuracy (%)			
	C4.5 Decision Tree	Random Forest	Naive Bayes	Bayes Net
1	62	60	56	64
2	80	80	86	84
3	92.5	89	91	90
4	96	92	94	92
5	98	96	96	95
6	98	97	96	95
7	97	97	96	94
8	96	96	95	93
9	96	96	93	93
10	95	95	93	92
11	94	93	92	91
12	92	93	91	90

Table 8. Confusion matrix for decision tree with experimental data.

Category	Laminated	Delaminated Plate
LAM	49	1
DLAM	1	49

Summary of the classifier results:

Correctly classified instances	98 (98%)
Incorrectly classified instances	2 (2%)
Kappa statistic	0.96
Mean absolute error	0.0296
Root mean squared error	0.1422
Relative absolute error	5.913%
Root relative squared error	28.4309%
Coverage of cases (0.95 level)	98%
Mean rel. region size (0.95 level)	50%
Total number of instances	100

The random forest algorithm produced a maximum accuracy of 96% with the top six features. The random forest randomly uses 10 trees as a forest and the maximum accuracy was predicted. Similarly, the selected naive Bayes and Bayes net algorithms were also used for the classification processes. The naive Bayes algorithm produced 96% as its maximum accuracy, whereas the Bayes net produced a maximum accuracy of 95%. Both algorithms produced the maximum accuracy with the top five contributing features.

4.5. Comparative Study

Table 9 shows the summarized results with both experimental and simulated time-domain signatures. Among the four algorithms considered, the decision tree produced the maximum accuracy on both simulated and experimental data with less processing time. Hence, the decision tree algorithm can be effectively used for identifying defective delaminated composite structures with minimal computation time. This motivates us to develop an OBD for displaying the results then and there. These results suggest that delamination can be identified using experimental and simulated vibration responses through the application of machine learning. Therefore, defects can be identified during the product development stage by studying the simulated signals. This will help researchers to eliminate structural defects in the laminated composites during initial stages of product development. This information will be useful for engineers to avoid catastrophic failure during the service period of a product.

Table 9. Comparative study.

Algorithm	Accuracy With Simulated Data	Time Taken to Build the Model (s)	Accuracy With Experimental Data	Time Taken to Build the Model (s)
Decision Tree	100	0.1	98	0.15
Random Forest	100	0.5	97	0.52
Naive Bayes	100	0.4	96	0.45
Bayes Net	100	0.6	95	0.6

5. Conclusions

A machine learning-based fault diagnosis has been proposed for identifying delamination in fiber-reinforced laminated structures. Glass fiber-reinforced rectangular laminate composite plates with and without delamination were considered to develop a finite element model. The forced vibration responses of the delaminated and laminated composite structures were acquired using an in-house developed finite element program using MATLAB®. The statistical information that was extracted from the forced vibration response was used to diagnose the damage in the laminated composite plates using machine learning algorithms. The greatest contributing features were identified from the extracted features using the attribute evaluator. The selected features were further classified using machine learning algorithms, such as decision tree, random forest, naive Bayes, and Bayes net algorithms for diagnosing the damage in the laminated structure.

The decision tree algorithm was found to be a computationally effective model in diagnosing the delamination of the composite structure. It was observed that the proposed model produced 98.5% accuracy in diagnosing the damage in the fabricated composite structure. Hence, this research work motivates us to develop an online prognostic and health monitoring module for detecting early damage to prevent catastrophic failures of structures.

Author Contributions: Conceptualization, S.G.; Methodology, J.R.; Software, L.J. and S.D.; Investigation, L.J., J.R. and Y.X.; Resources, S.M.; Writing – review & editing, S.R. and Y.X.; Supervision, L.J. and Y.X. All authors have read and agreed to the published version of the manuscript.

Funding: This research was funded by Vellore Institute of Technology (VIT) Chennai under VIT SEED GRANT and The APC was funded by VIT Chennai.

Institutional Review Board Statement: Not applicable.

Informed Consent Statement: Not applicable.

Data Availability Statement: Not applicable.

Acknowledgments: The authors thank the Management of, School of Mechanical Engineering, Centre for Automation, VIT Chennai and Cranfield University, Cranfield, UK, for their support in publishing this work. Additionally, the authors would like to thank the research scholar Atul, who helped acquire the signals.

Conflicts of Interest: The authors declare no conflict of interest.

References

1. Marjanovic, M.; Vuksanovic, D. Layerwise solution of free vibrations and buckling of laminated composite and sandwich plates with embedded delaminations. *Compos. Struct*. **2014**, *108*, 9–20.
2. Sha, G.; Radzienski, M.; Soman, R.; Cao, M.; Ostachowicz, W.; Xu, W. Multiple damage detection in laminated composite beams by data fusion of Teager energy operator-wavelet transform mode shapes. *Compos. Struct.* **2020**, *235*, 111798.
3. Doherty, J.E. *Nondestructive Evaluation, Chapter 12 in Handbook on Experimental Mechanics*; Kobayashi, A.S., Ed.; Society for Experimental Mechanics Inc.: Englewood Cliffs, NJ, USA, 1987.
4. Zhang, Z.; He, M.; Liu, A.; Singh, H.K.; Ramakrishnan, K.R.; Hui, D.; Shankar, K.; Morozovb, E.V. Vibration-based assessment of delaminations in FRP composite plates. *Compos. Part B Eng.* **2018**, *144*, 254–266.
5. He, M.; Ramakrishnan, K.R.; Wang, Y.; Zhang, Z.; Fu, J. A combined global-local approach for delamination assessment of composites using vibrational frequencies and FBGs. *Mech. Syst. Signal Proc.* **2022**, *167*, 108577.
6. Nikbakht, M.; Yousefi, J.; Toudeshky, H.H.; Minak, G. Delamination evaluation of composite laminates with different interface fiber orientations using acoustic emission features and micro visualization. *Compos. Part B Eng.* **2017**, *113*, 185–196.
7. Demi, A.; Hongping, Z.; Luo, H.; Wang, C. Mechanical impedance based embedded piezoelectric transducer for reinforced concrete structural impact damage detection: A comparative study. *Constr. Build Mater.* **2018**, *165*, 472–483.
8. Kessler, S.; Spearing, S.; Soutis, C. Damage detection in composite materials using Lamb wave methods. *Smart Mater. Struct.* **2002**, *11*, 269–278.
9. Dawood, T.A.; Shenoi, R.A.; Sahin, M. A procedure to embed fibre Bragg grating strain sensors into GFRP sandwich structures. *Compos. A Appl. Sci. Manuf.* **2007**, *38*, 217–226.
10. He, M.; Zhang, Z.; Ramakrishnan, K.R. Delamination Identification for FRP composites with emphasis on frequency-based vibration monitoring-a review. *SDHM Struct. Durab. Health Monit.* **2018**, *12*, 213–256.
11. Mohamad, H.M.G.; Wan, R. Vibration Analysis for Machine Monitoring and Diagnosis: A Systematic Review. *Shock. Vib.* **2021**, 9469318, 1-25. https://doi.org/10.1155/2021/9469318
12. Dorantes, J.J.S.; Delgado, M.P.; Redondo, J.A.O.; Rios, R.A.O.; Troncoso, R.D.J.R. Multiple-fault detection methodology based on vibration and current analysis applied to bearings in induction motors and gearboxes on the kinematic chain. *Shock. Vib.* **2016**, *2016*, 1–13.
13. Nobre, I.M.; Nicolini, J.L.; Garcia, J.D.; Mosso, M. Signal Processing technique for time domain measurement of S-Parameters. *J. Microw. Optoelectron. Electromagn. Appl.* **2016**, *15*, 105–114.
14. Reinhold, I. *Spectral Analysis for Signal Detection and Classification: Reducing Variance and Extracting Features*; Lund University: Lund, Sweden, 2021.
15. Marco, C.; Ahmed, E. On the LoRa modulation for IoT: Waveform properties and spectral analysis. *IEEE Internet Things J.* **2019**, *6*, 8463–8470.
16. Obaidi, A.A.R.; Towsyfyan, H. An experimental study on vibration signatures for detecting incipient cavitation in centrifugal pumps based on envelope spectrum analysis. *J. Appl. Fluid Mech*. **2019**, *12*, 2057–2067.

17. Talab, A.M.; Awang, S.; Ansari, M.D. A Novel Statistical Feature Analysis-Based Global and Local Method for Face Recognition. *Int. J. Opt.* **2020**, *2020*, 1–17.
18. Khairnar, A.; Patange, A.; Pardeshi, S.; Jegadeeshwaran, R. Supervision of carbide tool condition by training of vibration-based statistical model using boosted trees ensemble. *Int. J. Perform. Eng.* **2019**, *17*, 229–240.
19. Bansal, A.; Ravinder, A.; Sharma, R.K. Statistical Feature Extraction Based Iris Recognition System. *Sadhana Acad. Proc. Eng. Sci.* **2016**, *41*, 507–518.
20. Li, W.; Zhu, Z.; Fan, J.; Gongbo, Z.; Guoan, C. Fault diagnosis of rotating machinery with a novel statistical feature extraction and evaluation method. *Mech. Syst. Signal Proc.* **2015**, *50*, 414–426.
21. Song, F.; Zhongwei, G.; Dayong, M. Feature Selection Using Principal Component Analysis. In Proceedings of the 2010 International Conference on System Science, Engineering Design and Manufacturing Informatization, Yichang, China, 12–14 November 2010; Volume 1, pp. 27–30.
22. Khalid, S.; Tehmina, K.; Shamila, N. A survey of feature selection and feature extraction techniques in machine learning. *J. Sci. Conf. Proc*. **2014**, 372–378. https://doi.org/10.1109/SAI.2014.6918213
23. Sugumaran, V.; Muralidharan, V.; Ramachandran, K.I. Feature selection using decision tree and classification through proximal support vector machine for fault diagnostics of roller bearing. *Mech. Syst. Signal Proc.* **2007**, *21*, 930–942.
24. Gul, A.; Eşref, A. A feature selection algorithm for IDS. *Int. J. Comput. Sci. Eng.* **2017**, 816–820. https://doi.org/10.1109/UBMK.2017.8093538
25. Priyam, A.; Abhijeeta; Gupta, R.; Rathee, A.; Saurabh, S. Comparative analysis of decision tree classification algorithms. *Int. J. Curr. Eng. Technol.* **2013**, *3*, 334–337.
26. Li, G.; Huanxin, C.; Yunpeng, H.; Jiangyu, W.; Yabin, G.; Jiangyan, L.; Haorong, L.; Ronggeng, H.; Hang, L.V.; Jiong, L. An improved decision tree-based fault diagnosis method for practical variable refrigerant flow system using virtual sensor-based fault indicators. *Appl. Therm. Eng.* **2018**, *129*, 1292–1303.
27. Jegadeeshwaran, R.; Sugumaran, V. Comparative study of decision tree classifier and best first tree classifier for fault diagnosis of automobile hydraulic brake system using statistical features. *Measurement* **2013**, *46*, 3247–3260.
28. Aker, E.; Mohammad, L.O.; Veerapandiyan, V.; Ishak, B.A.; Noor, I.A.W.; Hashim, H. Fault detection and classification of shunt compensated transmission line using discrete wavelet transform and naive bayes classifier. *Energy J.* **2020**, *13*, 243.
29. Kiran, V.; Hemantha, K.; Gangadharan, K.V. Engine gearbox fault diagnosis using empirical mode decomposition method and Naive Bayes algorithm. *Sādhanā* **2017**, *42*, 1143–1153.
30. Kaplan, K.; Yılmaz, K.; Melih, K.; Mehmet, R.M.; Metin, E.H. An improved feature extraction method using texture analysis with LBP for bearing fault diagnosis. *Appl. Soft Comput.* **2020**, *87*, 106019.
31. Ozlem, A.; Oguz, G. Classification of multispectral images using Random Forest algorithm. *J. Geod. Geoinf. Sci.* **2012**, *1*, 105–112.
32. Paul, A.; Mukherjee, D.P.; Das, P.; Gangopadhyay, A.; Chintha, A.R.; Kundu, S. Improved random forest for classification. *IEEE Trans. Image Proc.* **2018**, *27*, 4012–4024.
33. Gomes, G.F.; Cunha, S.S.; Ancelotti, A.C. A sunflower optimization (SFO) algorithm applied to damage identification on laminated composite plates. *Eng. Comput*. **2019**, *35*, 619–626.
34. Lingyu, Y.U.; Zhaoyun, M.A. Various types of defects detection in flat and curved laminated composite plates using non-intrusive Lamb wave system. *J. Nondestruct. Eval. Diagn. Progn. Eng. Syst.* **2021**, *4*, 021008.
35. Khatir, S.; Samir, T.; Cuong, L.T.; Tinh, Q.B.; Magd, A.W. Damage assessment in composite laminates using ANN-PSO-IGA and Cornwell indicator. *Compos. Struct.* **2019**, *230*, 111509.
36. Jakkamputi, L.; Vasudevan, R. Dynamic Characterization of a CNT Reinforced Hybrid Uniform and Non-uniform Composite Plates. *Steel Compos. Struct.* **2019**, *30*, 31–46.
37. Arumugam, A.B.; Vasudevan, R. Dynamic instability analysis of rotating delaminated tapered composite plates subjected to periodic in-pane loading. *Arch. Appl. Mech*. **2016**, *86*, 1965–1986.
38. Reddy, J.N. *Mechanics of Laminated Composite Plates and Shells*; CRC Press: New York, NY, USA, 2003; pp. 132–139.



https://dspace.org/

Experimental and computational vibration analysis for diagnosing the defects in high performance composite structures using machine learning approach

Jakkamputi, Lakshmipathi; Devaraj, Saravanakumar; Marikkannan, Senthilkumar; Gnanasekaran, Sakthivel; Ramasamy, Sivakumar ...

2022-11-26
MDPI
https://doi.org/10.3390/app122312100
Jakkamputi L, Devaraj S, Marikkannan S, et al., (2022) Experimental and computational vibration analysis for diagnosing the defects in high performance composite structures using machine learning approach, Applied Sciences, Volume 12, Issue 23, November 2022, Article number 12100

Downloaded from a DSpace repository. https://dspace.org/